16. Velocity Effects in Fracture

H. SCHARDIN

Weil am Rhein, Germany

ABSTRACT

Fracture velocities may be measured with various techniques, including high-speed photography, schlieren optical methods, and ultrasonic techniques, as described in this chapter. Velocity measurements for different kinds and shapes of specimens under different loading conditions provide information on the physical phenomena controlling the fracture process. Glasses exhibit a constant maximum fracture velocity independent of temperature and stress. The plastics tested exhibit different velocities, but each velocity observed appears to be stable.

Introduction

This chapter summarizes recent work done at the Research Laboratory at Saint-Louis, France, and in the Department of Applied Physics at the University of Freiburg, Germany. The collaborators concerned with fracture problems are principally H. Hänsel and W. Struth (Saint-Louis) and F. Kerkhof (Freiburg). The hitherto existing publications and documents of this group are listed at the end of the paper.[1–51]

Experimental Methods

The Use of High-Speed Photography

Because the separation of the material in front of a fracture is normally connected with high velocities and therefore not easy to explore, we do not know very much about the physical process of fracture itself. It is obvious that high-speed photography should be applied. By this means, Schardin and Struth [1,2] found in 1937 the constant maximum fracture velocity in glass. The *multiple-spark camera* was used in this case, and it is still a very useful instrument. The necessary frame rates between

about 10^5 and 10^6 per second are very easy to realize, together with good spatial resolution. Usually, only phenomena in transparent plates are examined with the multiple-spark camera, but, by use of the light reflected from a good plane surface, nontransparent materials may be tested too.

The simple illumination of a transparent plate with point sparks and without other optical arrangements usually makes the front of the running fracture visible. This method indicates that the opening of the fracture is a sudden phenomenon. Only in the case of a very small stress, just sufficient to maintain the fracture, does the visibility become poor.

Optical Methods

To find the interior stresses connected with a propagating fracture, the following optical methods have been used:

(*a*) The Toepler-schlieren method, which indicates the deviation of the light transmitted by the plate. The deviation itself depends upon the angle of inclination of both surfaces at the point in question and also upon the density gradient in the plate if that factor is sufficiently large.

(*b*) The schlieren method with point light source (shadow method). It is sometimes better to use this simpler arrangement, which, to a first approximation, makes visible all points in the object where the deviation of the transmitted light changes.

(*c*) For mirrorlike surfaces of opaque materials, both methods may be used. Then only the deformation of one surface is tested; this is important in the study of bending waves. By using schlieren systems to study the transmitted and the reflected light at the same time, the difference of the behavior of both surfaces may be studied.

(*d*) The double-refraction system, which indicates the difference of both principal stresses. Together with the Toepler-schlieren method, which indicates primarily the sum of both principal stresses, this system should make it possible to determine the absolute values of the stresses.

(*e*) The interferometer method. At Freiburg an interferometer has just been installed to study running fractures in parallel glass plates.

Use of Ultrasonics

Even with the aid of high-speed photography, it is impossible to study phenomena that occur in the interior of an opaque material. Although a transparent specimen may have surfaces other than planes, the optical methods nevertheless become difficult.

In order to investigate the temporal behavior of a fracture process in such cases, the ultrasonic method was developed (Kerkhof and others [11,15,17,29,39,40]). The basis for this method is found in the well-known Wallner lines, but, instead of utilizing the statistical appearance of transverse waves which form these lines, the fracture surface is modulated

by well-defined, continuously emitted ultrasonic waves. Thus, the fracture surface contains time marks, and the real fracture process can be subsequently reconstructed. (The frequencies that are necessary are between about 10^6 and 10^7 cps.)

The first ultrasonics transmitter was placed, along with the specimen, into water. Today, two new arrangements have been developed by Manitz.[49] The first transmitter (Fig. 1), a usual *X*-cut quartz, transmits its energy in longitudinal waves into a water transducer enclosed by a

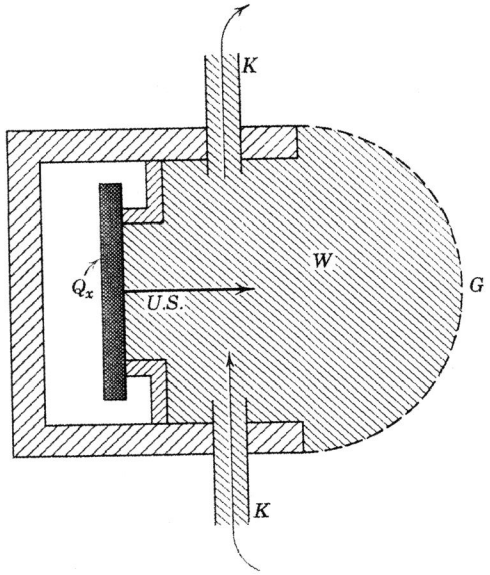

Fig. 1. Arrangement of an ultrasonic transducer transmitting longitudinal waves into solid samples by a water cushion. Q_x = *X*-cut quartz, *G* = rubber membrane, *W* = water, *K* = tubes for water-cooling, and *U.S.* = emitted longitudinal wave.

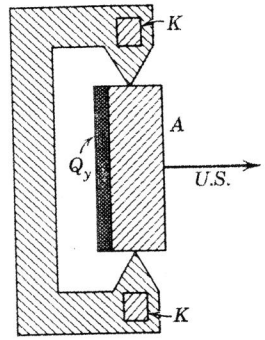

Fig. 2. Arrangement of a sound transducer generating transverse ultrasonic waves. Q_y = *Y*-cut quartz, *A* = compound oscillator with aluminum, *K* = cooling water jacket, and *U.S.* = emitted transverse wave.

rubber membrane. When the water contacts the specimen, the sound enters as well as if the whole sample were immersed in water. Water also serves as a cooling liquid which, by means of a small pump, circulates in a closed system through the tubes *K*. In this way, an ultrasonic wave can be transmitted to the rubber-sample interface at angles of incidence ranging from 0° to 40°.

The sound transducer mounting in Fig. 2 contains a transverse compound oscillator. At frequencies of about 5×10^6 cps (ordinarily used at Freiburg), the *Y*-cut quartz producing the transverse waves has a

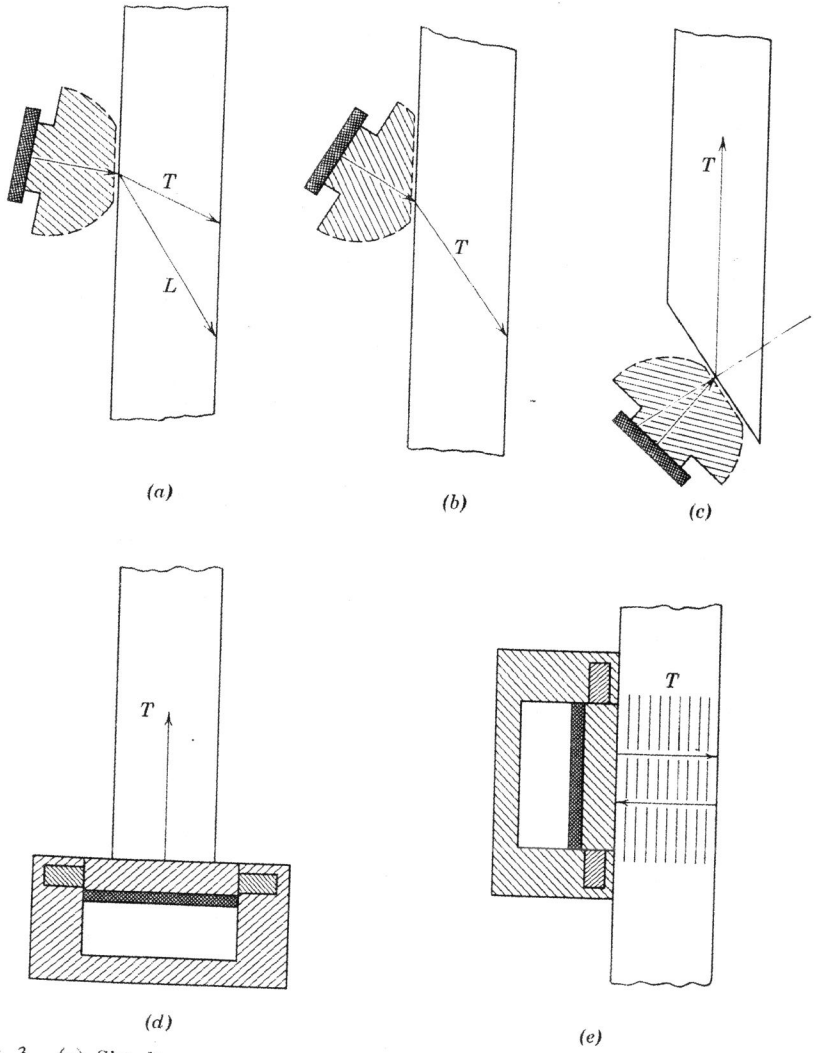

Fig. 3. (*a*) Simultaneous transmission of a longitudinal L and a transverse wave T into a test sample by means of a sound transducer with water cushion. (*b*) Transmission of a transverse wave T into a sample by a water transducer. Total reflection of the longitudinal wave in the transducer. (*c*) Transmission of a transverse wave T into a test rod in axial direction by a water transducer. (*d*) Transverse wave T transmitted into a specimen in axial direction by a compound oscillator with Y-cut quartz. (*e*) Standing transverse waves T transmitted into a test rod by a compound oscillator with a Y-cut quartz.

thickness of only 0.3 mm and can therefore be damaged easily. To avoid this, the crystal is cemented to an aluminum piece, the thickness of which is ten times the transverse wavelength (about 6.1 mm). Because of the intense heating during operation, the compound oscillator is also cooled by water passing through the channels K.

By means of such a mounting, it is possible to transmit transverse waves directly into the test sample, but only in a direction normal to the surface. Different arrangements are possible, as shown in Figs. 3*a* to *e*.

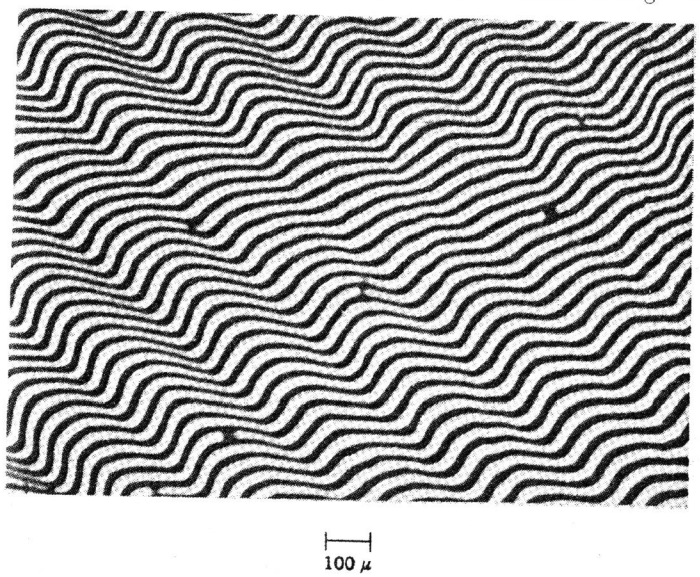

Fig. 4. Ultrasonic-modulated fracture surface, observed by an interference microscope (λ = 5461 Å). Sound frequency: 5.029×10^6 cps, fracture velocity $\sim$ 1200 m/sec. Depth of lines: 0.2 to 0.8 μ.

The ultrasonic-modulated fracture surface can be investigated by (*a*) a simple microscope, (*b*) a schlieren-microscope, or (*c*) an interference-microscope. Figure 4 demonstrates that the fracture surface directly follows the variation of the ultrasonic stresses. Figure 5 is an example of good ultrasonic fracture lines in glass, from which fracture velocity can be determined. The velocity is different in each part of the cross section. Figure 6 shows a photograph of the modulated fracture surface in Plexiglas; the frequency of the ultrasonic waves (5×10^6 cps) is somewhat high with respect to the low fracture velocity (170 to 210 m/sec).

Loading

To be able to study velocity effects in fracture with the multiple-spark camera, it is necessary to obtain convenient synchronization between the

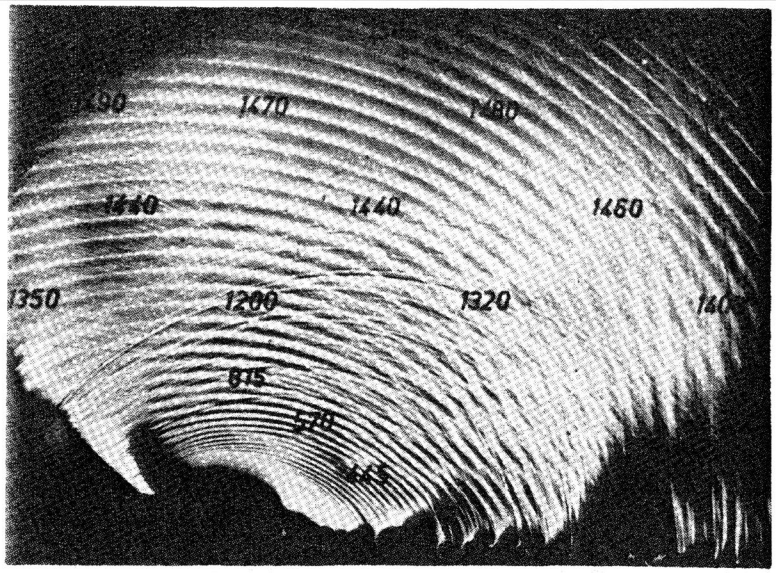

Fig. 5. Fracture face modulated by ultrasonic and Wallner lines.

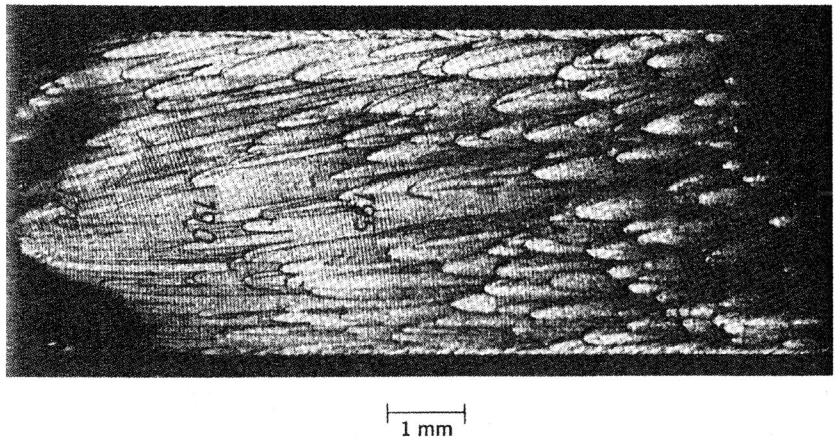

Fig. 6. Fracture face of Plexiglas rod with transverse ultrasonic waves. Fracture starts at the left side of the frame. Numbers give fracture velocity in m/sec.

loading and the available working time of the camera. This is easily done for ballistic or impulse loading, for example, by allowing a projectile to strike the edge of a plate or to penetrate the center of the plate. In the same way, one may use small charges of a primary explosive such as lead azide. However, stresses transmitted in this way are generally extremely

high and of a complicated distribution. Although a great deal of information about fracture could be obtained by means of ballistic loading, it is also necessary to use classical loading methods, which usually entail tensile testing. Particular arrangements are necessary to guarantee very high or very low loading velocities.

One system used by the author to obtain high loading velocities is shown in Fig. 7. A weight falling on a plate transmits stress to the specimen.

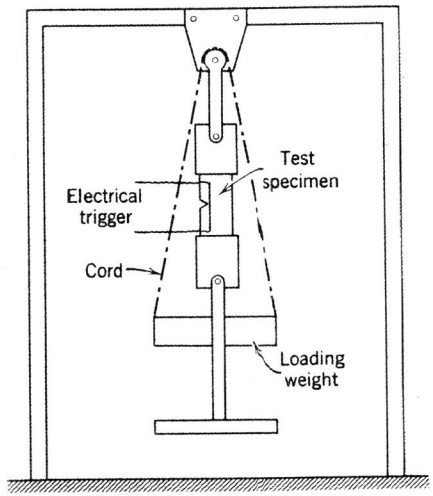

Fig. 7. Experimental arrangement for a tensile test by means of a falling weight.

Initial Phase of a Fracture

After this short description of the experimental methods, results concerned with velocity effects in fracture can now be discussed. With the exception of ballistic loading, the fracture starts with a low velocity. The ultrasonic method described is the best tool to study this first phase of the fracture. If we look at Figs. 5 and 6, where some velocity values are indicated, we find that the velocity increases with the distance from the origin of the fracture. This result agrees with those published by Smekal.[52] In Fig. 8, fracture velocities are plotted as a function of distance.

When the fracture starts with low velocities, the time for the first phase of the phenomenon may be very long. Approximately up to the turning point of the curve in Fig. 8, the elastic energy released by the running fracture is not sufficient to maintain the fracture. Energy must be added by the statistical fluctuation of heat energy. This takes time

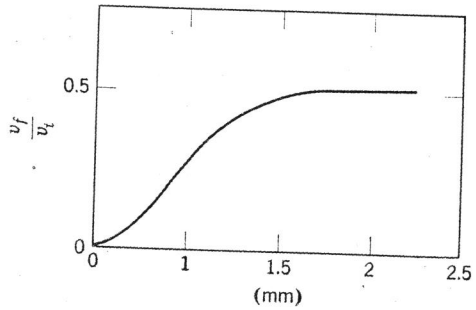

Fig. 8. The increase of velocity in the initial phase of a fracture up to a constant maximum value. v_f is the fracture velocity. v_t is the velocity of the transverse wave.

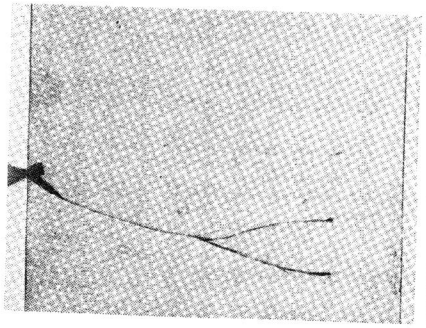

Fig. 9. Fracture in glass plate produced by striking knife edge at left. Load increases from Figs. 9 to 12.

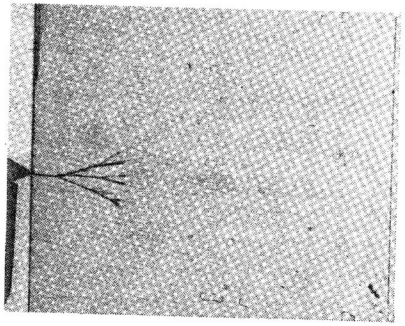

Fig. 10. Fracture in glass plate produced by striking knife edge at left. Load increases from Figs. 9 to 12.

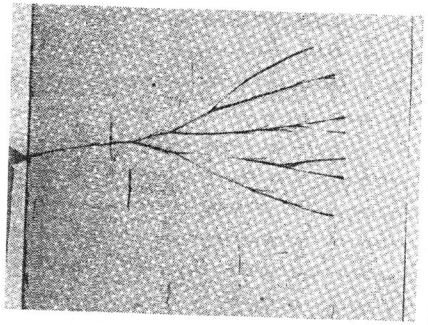

Fig. 11. Fracture in glass plate produced by striking knife edge at left. Load increases from Figs. 9 to 12.

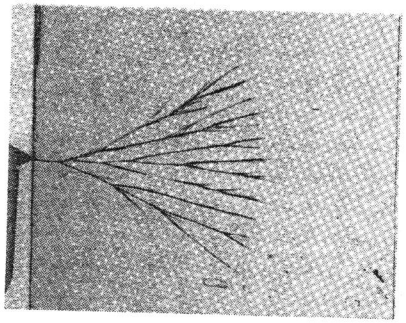

Fig. 12. Fracture in glass plate produced by striking knife edge at left. Load increases from Figs. 9 to 12.

and results in low fracture velocity. At a later stage, when elastic energy is able to maintain the fracture, thermal effects play no part. Velocity increases up to a limit, which is the constant final fracture velocity in the ideal brittle case.

For a long time, the initial phase of the fracture could not be revealed by use of high-speed photography. The reason is mainly that triggering cannot be realized precisely at the beginning of a fracture. Therefore,

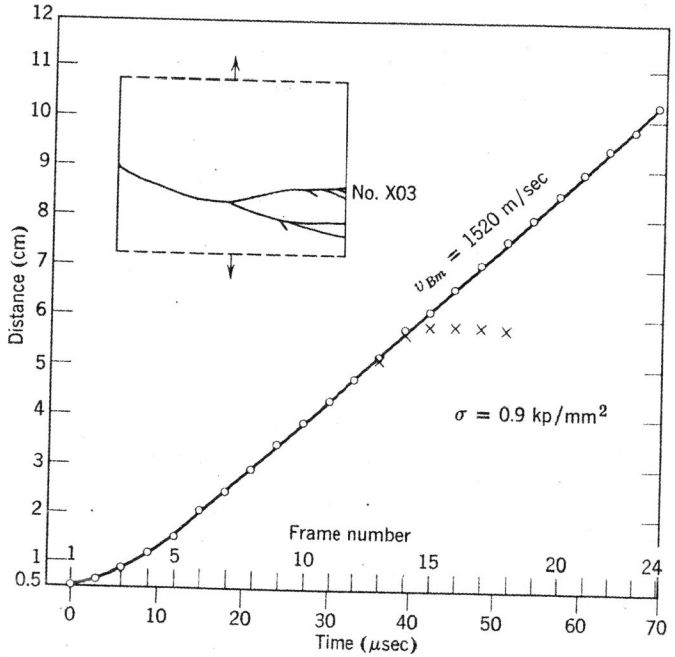

Fig. 13. Evaluation of a complete series of multiple-spark photographs of a fracture similar to those of Figs. 9 to 12.

it was necessary to enlarge the distance between the origin and the point of full velocity. For this purpose, a tensile machine was applied which allows the stress to rise very slowly and which works without oscillation. It was possible, consequently, to obtain in glass plates a sufficiently long initiating phase of the fracture. The start of the fracture was produced by striking a knife edge against the edge of the plate. The multiple-spark camera was triggered at this moment by an electrical contact. Figures 9 to 12 show four different fracture formations under increasing loading. Figure 13 indicates the time-distance evaluation for one complete series. In the initial phase, the fracture velocity grows to its constant maximum value. Only this initial phase is plotted in Fig. 14 for

three fractures, which are indicated in the figure. We see that, with higher tensile stress at the moment of fracture, more bifurcations occur and the initial zone decreases.

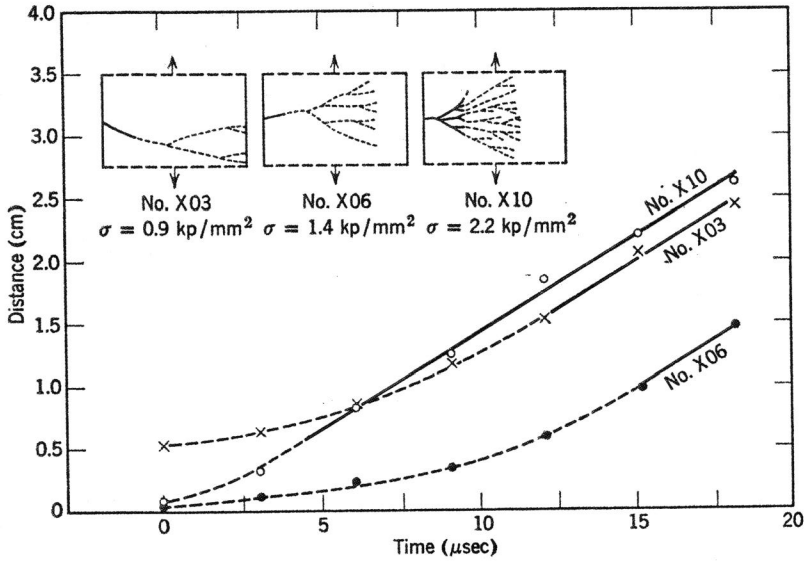

Fig. 14. The initial phase of fracture for three fractures at increasing values of stress.

Constant Maximum Fracture Velocity in Brittle Materials

In 1937, Schardin and Struth [1,2] found the astonishing fact that the fracture velocity for glass is a constant (1500 m/sec for normal glass; Fig. 15). At once, the questions arose: On what does this velocity depend, and how is it caused?

At first, temperature seemed to have no effect. New experiments made by Dimmick [53] in 1951 with better precision gave a low *negative* gradient,

$$\frac{1}{v_f}\frac{dv_f}{dT} \approx -10^{-4}/^{\circ}\mathrm{K}$$

This demonstrates that the physical phenomenon of fracture at this high velocity has nothing to do with heat; it is really an athermic process.

Another question was: Is the maximum velocity influenced by the over-all stress at the moment of the fracture, at least a little? Securit glass plates with high internal stresses gave exactly the same velocity as identical plates from which stresses had been removed. Recently, ex-

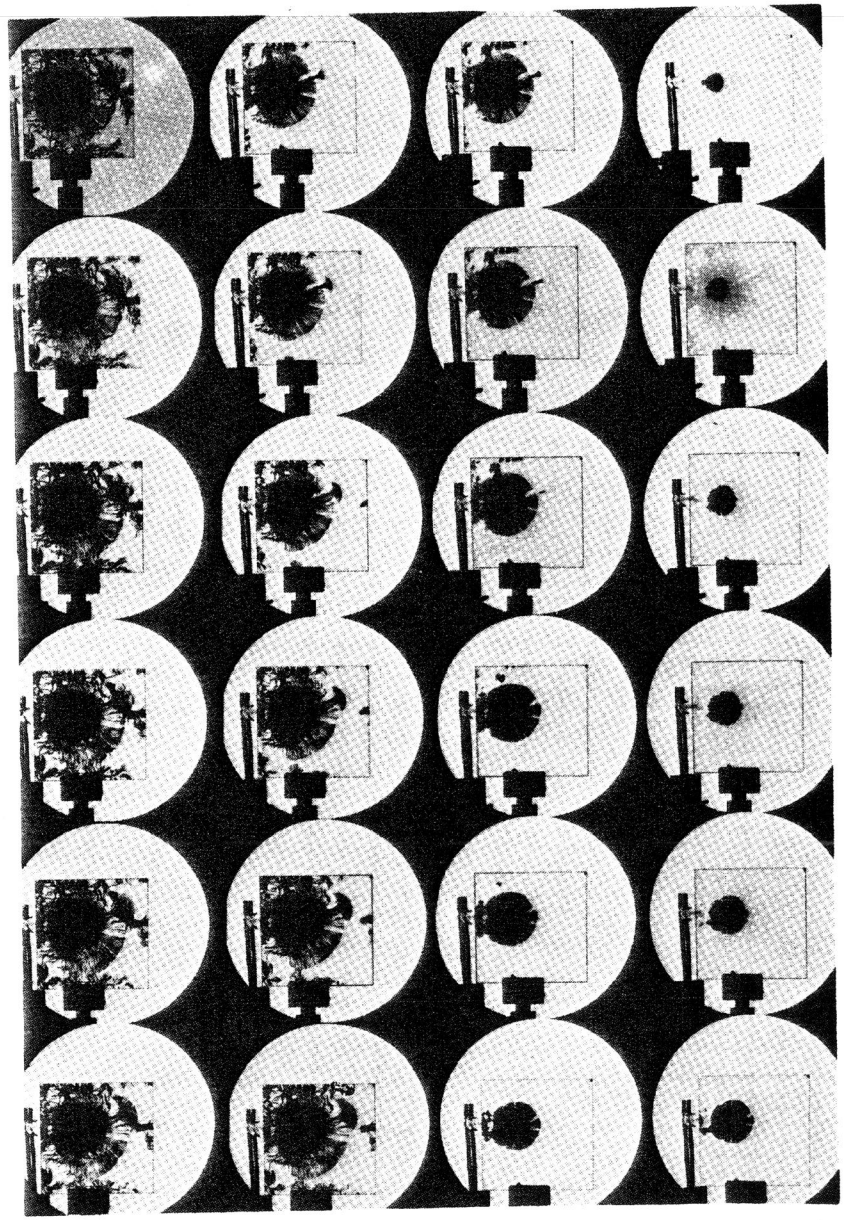

Fig. 15. Successive stages of a fracture in glass. Fracture initiated by a striking projectile. Fracture begins at upper-right corner.

periments have been carried out with glass plates under high compression load. Within the limit of experimental errors, no load effect could be detected.

It is, however, obvious that maximum fracture velocity depends on the material. Table 1 gives the composition of a large number of glasses for which the velocity has been measured by using the multiple-spark camera. Fracture was initiated by a striking projectile. The precision

TABLE 1. Composition of Glasses

No.	SiO_2	Na_2O $+K_2O$	PbO	BaO	B_2O_3	Al_2O_3	CaO	ZnO	Sb_2O_3	TiO_2	As_2O_3
				Glass Composition (%)							
				Flint Glasses							
1	78.7	12.4	8.8	0.1							
2	75.6	12.8	11.4	0.2							
3	75.7	10.5	13.5	0.3							
4	72.9	14.3	12.8								
5	72.7	10.4	16.7	0.2							
6	71.9	10.0	18.1								
7	70.9	9.8	18.8	0.5							
8	70.6	10.3	18.8	0.3							
9	69.7	10.2	19.8	0.3							
10	70.3	7.8	21.9								
11	68.2	8.2	23.4	0.2							
12	67.1	6.8	25.9	0.2							
13	66.0	6.2	27.6	0.2							
14	63.5	5.7	30.6	0.2							
15	60.8	5.9	33.1	0.2							
16	60.6	4.3	34.9	0.2							
17	57.1	2.4	40.5								
				Other Optical Glasses							
18	100										
19	69.1	8.2	0.1		11.2	2.5		8.8	0.1		
20	73.4	15.2		0.6	10.5		0.3				
21	61.0	11.4			17.7	9.9					
22	62.8	7.6			22.0	1.9			5.3		0.4
24	71.1	15.5	0.3		3.3		2.9	6.6			0.3
25	63.1	8.9	0.8	9.7	6.4			10.6	0.1		0.4
26	46.3			28.9	23.2	1.2			0.1		0.3
27	59.2			23.3	6.0	2.1		9.1			0.3
28	44.5			27.1	12.9	0.7	5.5	5.6	0.1	3.4	0.3
29	66.0	7.5	8.8	9.0				8.5			0.2

No.	SiO_2	Na_2O $+K_2O$	PbO	BaO	B_2O_3	Al_2O_3	CaO	ZnO	Sb_2O_3	TiO_2	As_2O_3
						Simple Glasses					
31	74.5	25.5 *									
32	75	20.5 *					4.5				
33	75	15 *					10				
34	75	10 *					15				
35	80	20 *									
36	70	20 *					10				
37	65	20 *					15				
38	75	15 *		10							
39	75	15 *						10			
40	75	15 †					10				
41	75	15 †		10							
42	65	15 *			10		10				

* No K_2O present.
† No Ma_2O present.

of the speed measurement is better than 1% when the propagation of the fracture is given by an exact circle, as shown in Fig. 15. Sometimes, however, the glass is so brittle that many secondary fractures appear; this reduces the observable length of a single fracture (Fig. 16). For a length of 1 cm, the accuracy is about 1%; for shorter lengths, the accuracy is correspondingly inferior.

For small diameters of the specimen, the direction of the fracture is strongly influenced by elastic waves; fractures therefore follow a curved path. Figure 17 shows a single picture from a series, and Fig. 18 the corresponding evaluation. Fracture Number 1 stops at the moment the two fractures (1*a* and 1*b*) turn together, but normal velocity is quickly re-established.

Whenever it is possible to measure the velocity, it is found to be constant under these given experimental conditions. The variation of the stress by the different elastic waves has no detectable influence. In Table 2, results of the fracture-speed measurements are compiled, together with some other material constants, such as

v_f = fracture velocity (m/sec)
ρ = density (g/cm³)
E = Young's modulus
μ = Poisson's ratio
v_t = velocity of the transverse wave
P_A = values for Plexiglas (Alsthom)
St = values for C steel

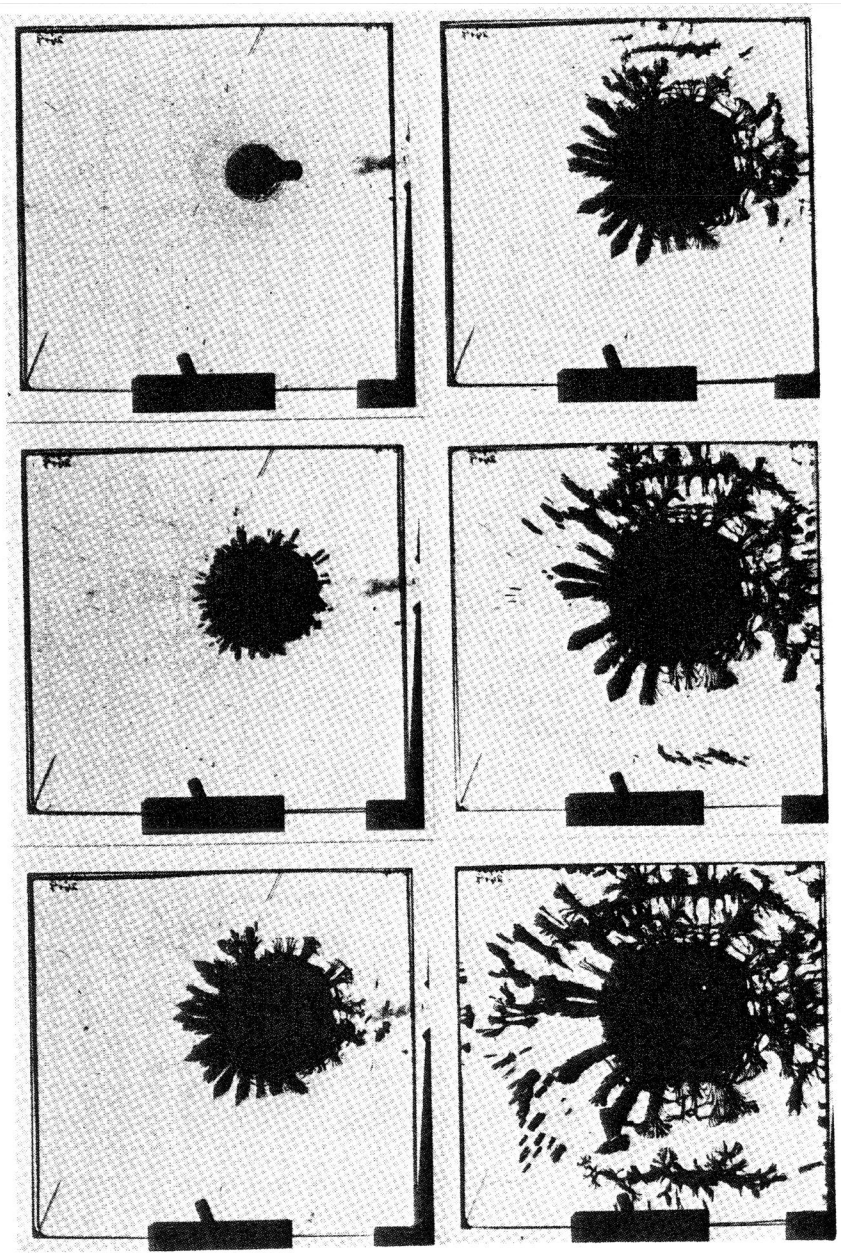

Fig. 16. Successive stages of a fracture in extremely brittle glass, showing occurrence of secondary fractures. Fracture begins at upper-left corner.

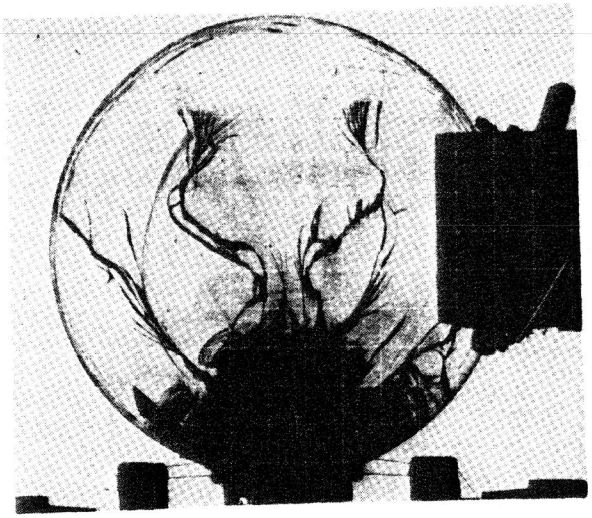

Fig. 17. Single picture from a series.

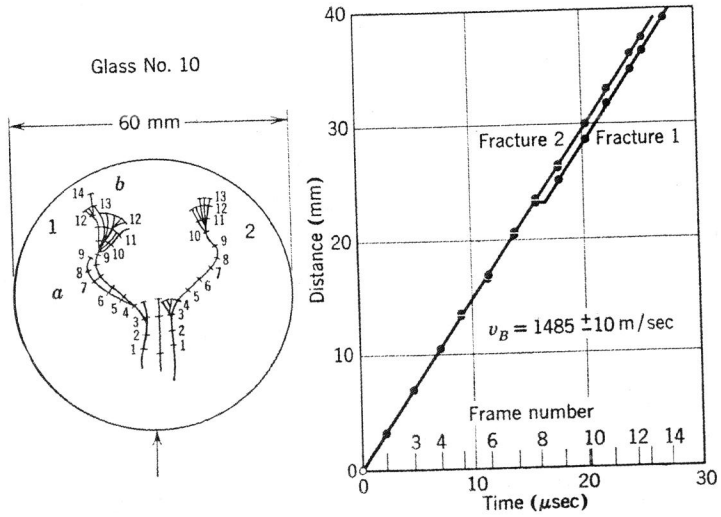

Fig. 18. Evaluation of the series of which Fig. 17 is a part. Fracture Number 1 stops a moment when fractures 1*a* and 1*b* are turning together.

TABLE 2. Fracture-Speed Measurements

No.	v_f (m/sec)	ρ (g/cm³)	E (kg/mm²)	μ	$(E/\rho)^{1/2}$ (m/sec)	v_t (m/sec)	v_f/v_t
1	1400	2.94	6199	0.2101	4550	2925	0.479
2	1340	3.12	5969	0.2150	4330	2780	0.482
3	1340	3.22	5941	0.2144	4255	2730	0.491
4	1260	3.22	6091	0.2235	4310	2755	0.457
5	1240	3.45	5579	0.2183	3985	2550	0.486
6	1190	3.51	6070	0.2290	4120	2625	0.453
7	1170	3.57	5847	0.2227	4010	2565	0.456
8	1140	3.59	5492	0.2211	3875	2480	0.460
9	1100	3.68	5751	0.2289	3915	2500	0.440
10	1090	3.78	5763	0.2246	-3865	2470	0.441
11	1045	3.91	5940	0.2298	3860	2460	0.425
12	1015	4.08	5808	0.2251	3735	2385	0.426
13	1000	4.21	5838	0.2281	3690	2355	0.425
14	905	4.43	5821	0.2330	3590	2285	0.396
15	850	4.62	5733	0.2360	3490	2220	0.383
16	840	4.80	5707	0.2387	3415	2170	0.387
17	750	4.79	5643	0.2400	3400	2160	0.347
18	2155	2.6	7630	0.17	5365	3510	0.614
19	1740	2.54	7146	0.2150	5255	3370	0.516
20	1705	2.53	7931	0.2070	5545	3570	0.478
21	1570	2.27	4712	0.2411	4515	2865	0.548
22	1540	2.54	5211	0.2240	4485	2865	0.538
24	1500	2.57	3722	0.2235	5285	3380	0.444
25	1345	3.11	7770	0.2450	4950	3135	0.429
26	1325	3.60	9094	0.2644	4980	3130	0.423
27	1220	3.55	8007	0.2659	4705	2955	0.413
28	1200	3.77	8712	0.2742	4760	2985	0.402
29	1150	3.49	6584	0.2433	4300	2730	0.412
P_A	305–655	1.18	535	0.35	2110	1285	0.237–0.510
St	963–1090	7.80	21000	0.28	5140	3210	0.300–0.340

The question now is whether any correlation exists between the fracture and the different elastic waves. To decide this, fracture velocity is plotted versus $(E/\rho)^{1/2}$. It can be seen from Fig. 19 that the experimental points scatter widely; this indicates that there is no exact correlation. Attempts have been made [54–56] to show theoretically that the maximum fracture velocity equals $0.5v_t$. Figure 19 proves that this relation can be regarded

only as an approximate one. The scatter of the measurements that are plotted, together with the straight line representing the supposed law $v_f = 0.5v_t$, exceeds distinctly the limits of experimental errors ($\pm 2\%$). Therefore, the statement of Bueche and White [57] that the rule $v_f = 0.5v_t$ is experimentally proved is not precisely founded. In particular, this rule predicts no direct influence of the chemical composition on fracture velocity. That fracture speed does depend on the chemical com-

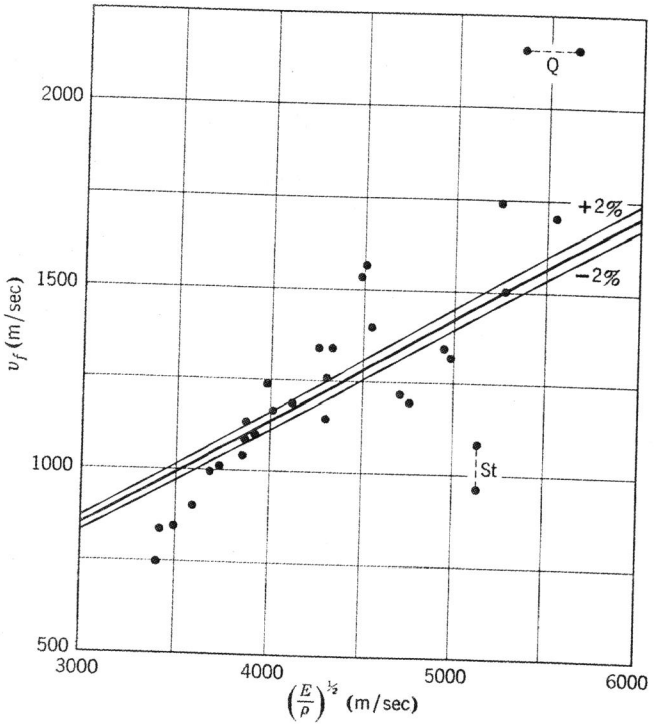

Fig. 19. v_f vs. $\sqrt{E/\rho}$ for different glasses.

position may be demonstrated by plotting the measured velocities in a three-material diagram (Hänsel).[42] Figure 20 shows as an example the system SiO_2-PbO-Na_2O/K_2O, where v_f/v_t and μ are plotted versus $(Na_2O + K_2O)/SiO_2$ and PbO/SiO_2.

The values for v_f/v_t and μ follow a regular curve in a satisfying manner. However, the ratio v_f/v_t is not equal to 0.5; in the range $0 < PbO/SiO_2 < 0.7$, it decreases in an approximately linear way from 0.53 to 0.35. It is supposed in this case that Na_2O and K_2O are interchangeable. Other similar plots could be added. We conclude that v_f

itself and the ratio v_f/v_t are functions of the chemical composition of the material and that v_f is a new physical constant of the material.

No doubt, mathematical relations can also be found between v_f and other physical constants that depend on the chemical composition, but such indirect correlations cannot essentially contribute to an understanding of the physical phenomena. It seems necessary to determine direct

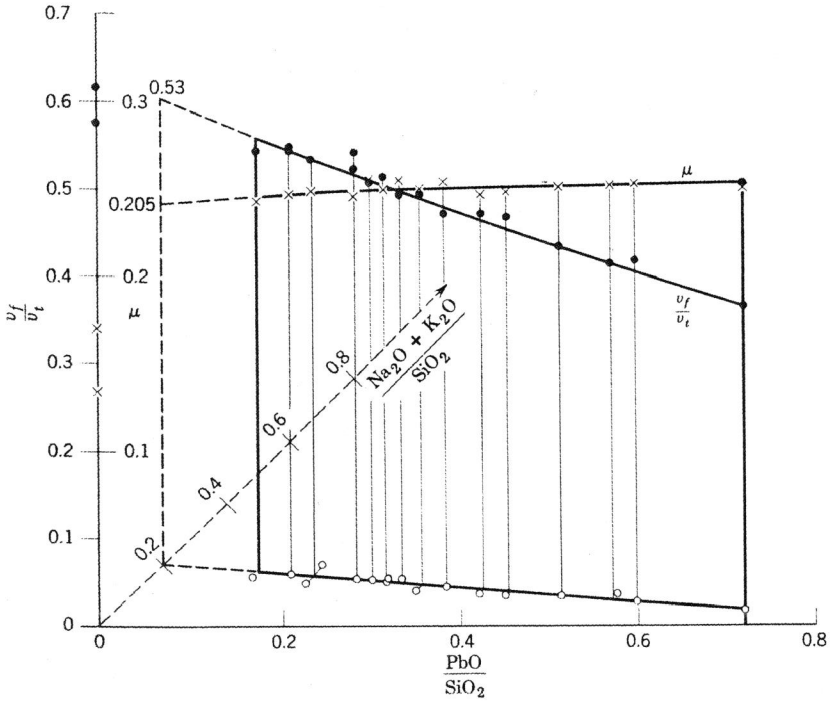

Fig. 20. v_f/v_t and μ in a three-material diagram.

relationships between physical values, but ones that would give greater accuracy than $v_f/v_t = 0.5$. One idea in this direction is that of Kerkhof: [51] At the front of a stationary running fracture, new surface energy is continuously created. Therefore, surface energy plays, to a certain extent, a part analogous to that of elastic energy in a normal elastic wave. It is consequently quite natural to suppose that fracture velocity is controlled by T/ρ (T = surface tension) as elastic waves are controlled by E/ρ, apart from the different dimensions. Macroscopic elastic phenomena do not seem to be so important to the microscopic events in the front of the fracture formation. Unfortunately, surface tensions for solid materials are not very well known, but, according to Ainsworth [58] and Taylor,[59]

a relation does exist between surface tension and microhardness σ_H. Therefore, we try to put

$$v_f = -A + B\sqrt{\sigma_H/\rho}$$

where A and B are positive constants.

Figure 21 shows the fracture velocity versus $\sqrt{\sigma_H/\rho}$ for some silicate glasses for which the microhardness could be estimated. The heavy straight line gives a good approximation for all velocity values; it corresponds to the equation

$$v_f = -560 + 2.48\sqrt{\sigma_H/\rho}$$

Though this explanation of the observed maximum fracture velocity is only an attempt, it seems of great interest.

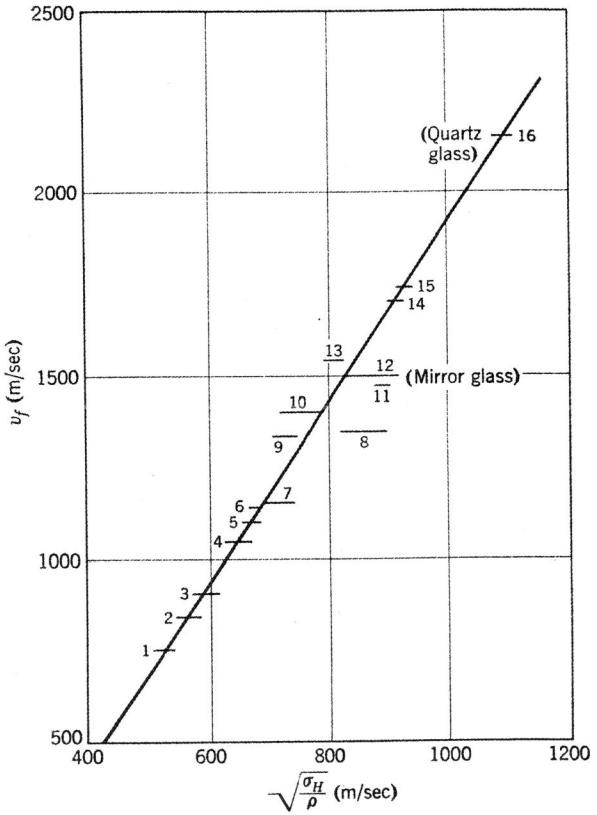

Fig. 21. Maximum fracture velocity as a function of $\sqrt{\sigma_H/\rho}$. σ_H = microhardness, ρ = density. Length of the short lines indicates the accuracy of each value.

In order to extend our understanding of the maximum velocity, we must principally consider the following kinds of energy: surface, kinetic, elastic, and plastic. Therefore, the fracture velocity should be determined by an equation of the form

$$v_f = f(T, \rho, E, \mu, X)$$

where X indicates the residual plastic energy in the material, which is not fixed by the other values. As long as it is not possible to establish a formula of this general type and to include in it a quantitative value for the plastic deformation, experiments will dominate the theory.

Demonstration of the Maximum Velocity by a Bursting Glass Tube

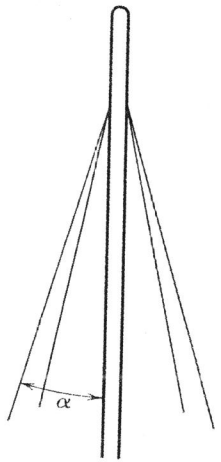

Fig. 22. Glass tube and shock wave formed during fracture.

A glass tube with one end closed is filled with compressed air, the pressure of which is increased until it bursts. The fracture starting from the "burst point" runs through the tube with the maximum velocity. Between the projected glass splinters, the air expands and forms a shock wave, the velocity of which is somewhat higher than the speed of sound. The angle α between the intact glass tube and the shock (Fig. 22) is given by

$$\sin \alpha = a/v_f$$

where a is the shock velocity and v_f is the fracture velocity.

Figure 23 shows three successive frames of this phenomenon. The angle α is 13°; if we use a value for a approximately equal to the velocity of sound, we find for the fracture velocity

$$v_f = 340/\sin 13° = 1500 \text{ m/sec}$$

which is in agreement with the results obtained for ordinary glass by other techniques.

Fracture Velocity in the Bending Test

It is well known that a bent bar has its maximum stress at the outer surface. A fracture can, nevertheless, penetrate into the interior. To study velocity effects in the bending test, a glass plate (44 mm wide, 9 mm

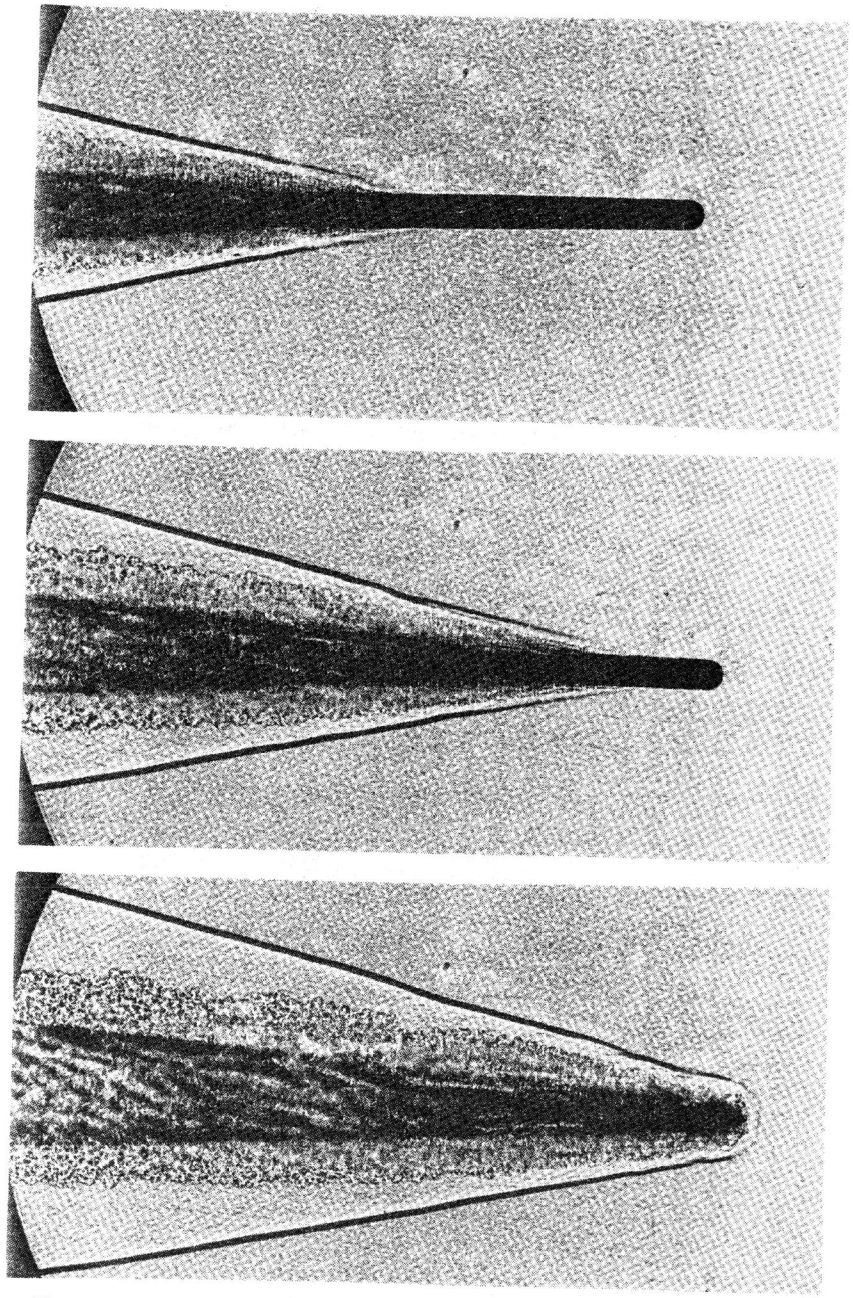

Fig. 23. Successive frames of shock wave formed during fracture of glass tube.

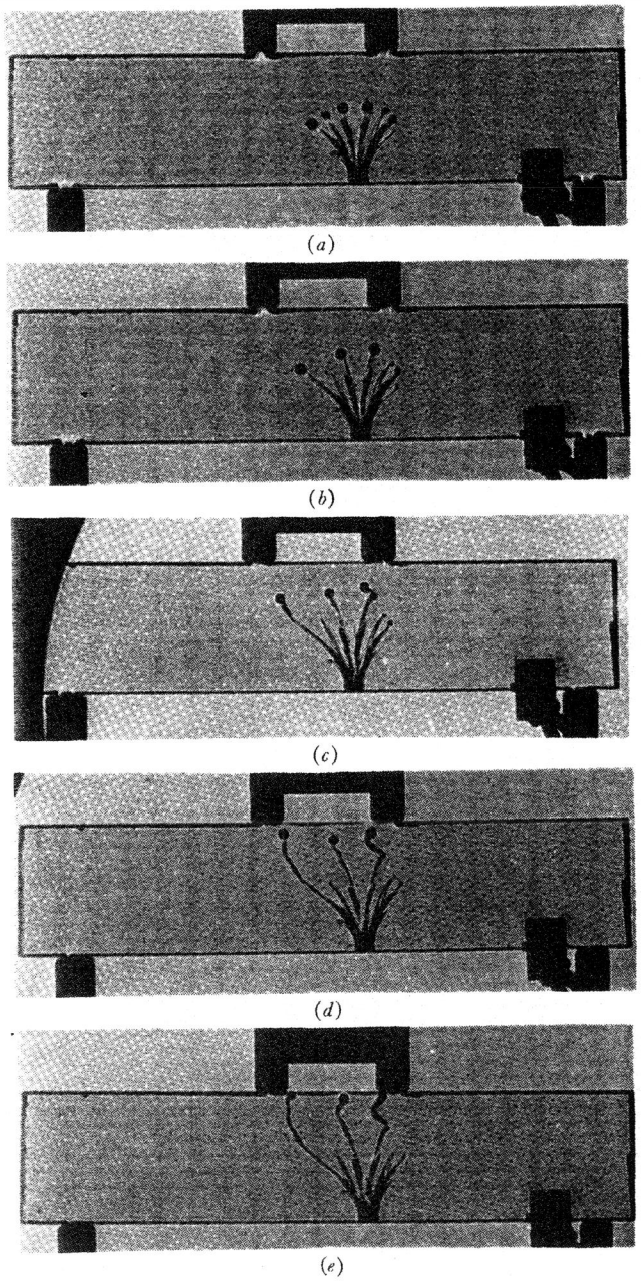

Fig. 24. Successive stages in the fracture of a bent glass plate.

thick, and 200 mm long) was bent in two-point loading (Figs. 24*a* to *e*). On the tension-side surface, a metallic layer was coated to trigger a multiple-spark camera at the start of the fracture. An optical arrangement was used to obtain a shadowgraph of the phenomenon. Figure 24*a* indicates that all single cracks are limited by a circle, which means that all cracks have the same velocity (except the one on the right, which has stopped). In Fig. 24*b*, only three cracks are still traveling. At the tip of each traveling crack, there is a black circle. The light, when passing this region, is deviated toward the outside, owing to the high stress concentration in front of the fracture. The diameter of this "stress corona" indicates the elastic energy available to maintain the fracture.

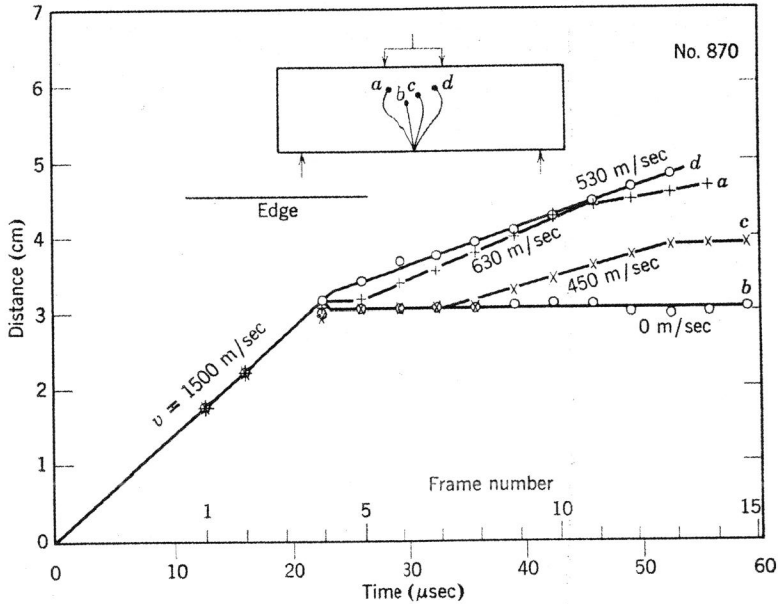

Fig. 25. Evaluation of a fracture similar to that shown in Fig. 24.

The distance-time evaluation of such a series leads to the astonishing conclusion (Fig. 25) that the maximum value for the fracture velocity is maintained beyond the neutral zone into the compression region. The traveling fracture is accompanied by its own kinetic energy (stress corona) which provides the fracture tension. When the elastic transverse wave, which starts with the fracture, is reflected from the other side and strikes the fracture front, the fracture velocity suddenly decreases to a lower value, which is determined by the deformation of the whole glass plate. Sometimes a change in direction of the fracture propagation is connected with the decrease of the velocity.

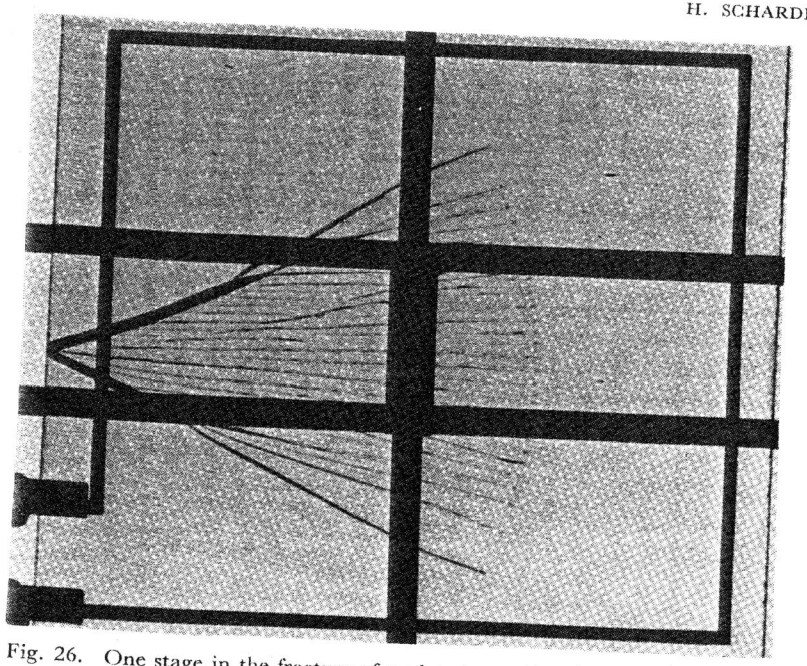

Fig. 26. One stage in the fracture of a plate bent about an axis in the plane of the plate.

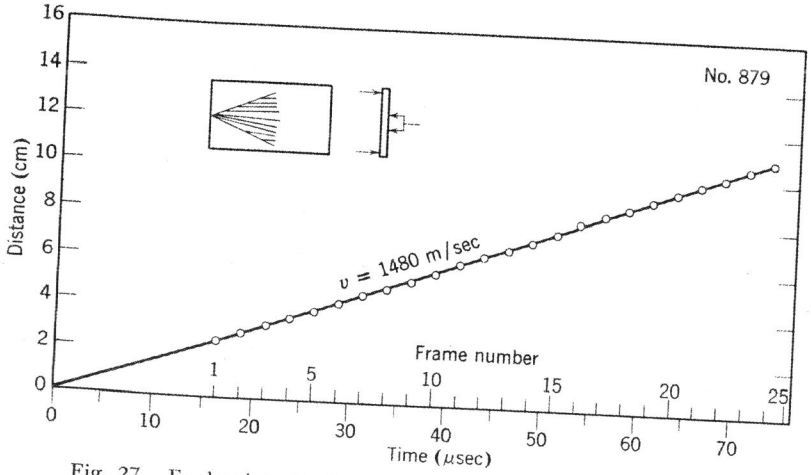

Fig. 27. Evaluation of a fracture similar to that shown in Fig. 26.

The experiment described demonstrates what happens in one cross section of a bent plate; but suppose that a whole plate is bent about an axis in the plane of the plate. This situation would raise a question as to whether the fracture, propagating in the tension region along the length of the plate, would be able to take along the fracture in the compression zone with the full velocity. Multiple-spark photographs have been taken in this case, too. Figure 26 shows one example, with the evaluation in Fig. 27. In this case, the full maximum fracture velocity is maintained. The evaluation for a fracture with one bifurcation (Fig. 28) gives a slightly different result: One branch has full velocity, but the other is a little slower. Therefore, the maximum velocity should not be determined by bending tests.

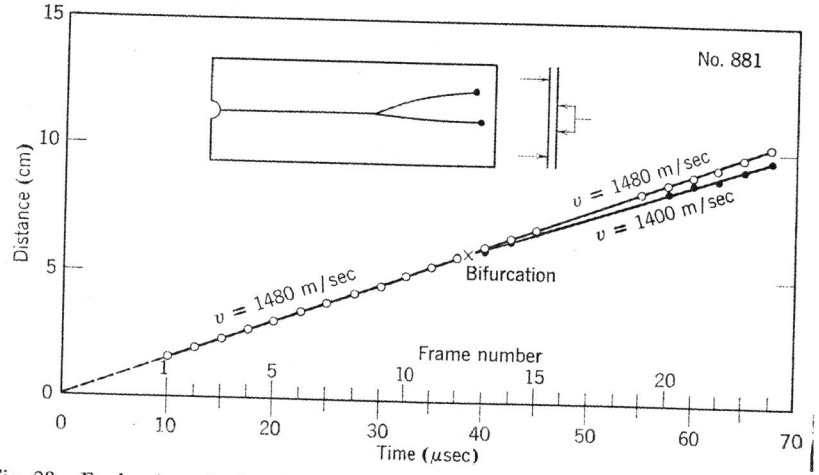

Fig. 28. Evaluation of a fracture similar to that shown in Fig. 26 but having only one bifurcation.

Fractures Propagating Apparently Faster than Maximum Velocity

When a glass plate has a scratch on its surface or a tension schliere in the interior, a crack will follow this line if the loading tension coincides approximately with this direction of propagation. Furthermore, secondary fractures can be initiated continuously some distance in front of the fracture. In this way, a higher fracture velocity than the normal maximum value is apparently realized. That this supervelocity is not a real fracture velocity is demonstrated by Fig. 29: Two supervelocity cracks are visible. Both are creating a great number of new fractures

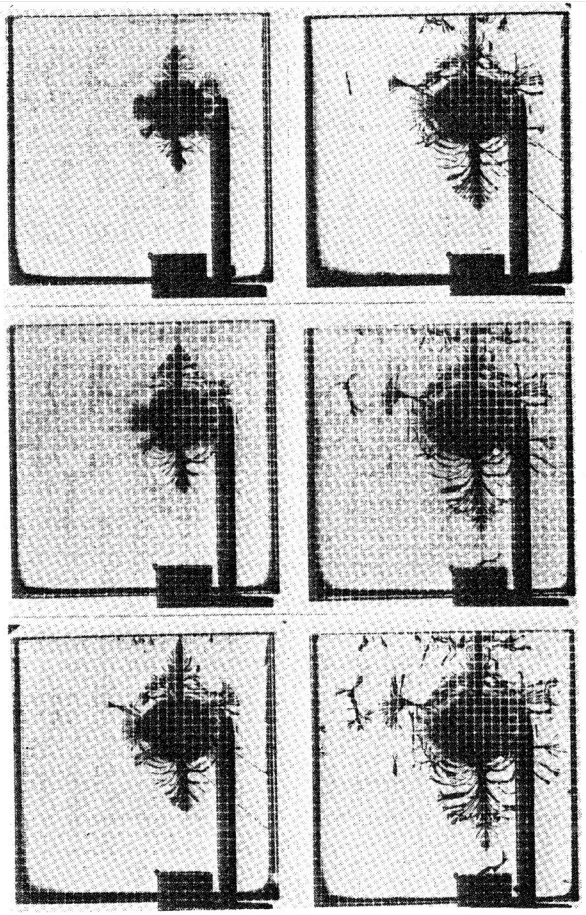

Fig. 29. Supervelocity cracks.

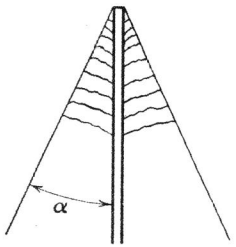

Fig. 30. Angle between supervelocity crack and the front of many normal-velocity cracks.

with normal velocity which start on both sides of the main fracture (Fig. 30). The angle α is determined by the relation

$$\sin \alpha = v_f / v_s$$

where v_f is the normal maximum velocity and v_s is the supervelocity. Secondary fractures a short distance in front of the primary fracture most often form hyperbolic lines by superposition of the two propagating fracture surfaces.

In materials in which plastic deformations occur

(for example, in Plexiglas), secondary fractures are formed continuously by a chain mechanism. The over-all propagation speed is, therefore, not accurately determined and depends to a high degree on the loading and the loading speed.

Decrease of the Fracture Velocity

It is an astonishing fact that during the twenty years that high-speed photography has been used to study fracture phenomena no continuous velocity decrease of a crack once running at maximum speed could be observed. Very often a crack stops rapidly, and no transition phase can be detected within the space and time resolution of the applied high-speed equipment (order of magnitude: 1 mm and 1 μsec, respectively). This is true for high-speed as well as for low-speed loading. It happens frequently that a fracture propagates discontinuously, but if it travels, it travels with full speed. Obviously, the average velocity may be reduced in this case. It may be that this fact has something to do with the existence of both surfaces, since high-speed investigations were concerned only with glass plates. On the other hand, it is surprising that the maximum velocity has exactly the same value in thin plates and in thicker samples. This would indicate that the surface does not influence the fracture process. The ultrasonic method would permit the study of this velocity effect in the interior of larger specimens.

It may be, however, that there is a fundamental reason for the non-existence of a gradual decrease of fracture velocity. When a fracture is running continuously at maximum speed, a certain value of kinetic energy is connected with the phenomenon. Therefore, in spite of a decrease in the exterior stress, the fracture may propagate for a certain period before consuming all of its own kinetic energy; then it stops abruptly because the exterior stress is too low to maintain the fracture.

The only condition under which a velocity decrease is observed by high-speed photography is when hackle marks appear. It is possible that in this case, as a result of the increase of surface energy, the fracture velocity decreases from the normal value to a lower one, as shown in an example published in 1954.[22] Similar results were obtained by the ultrasonic method for hackle marks.

In addition to the velocity effect, the interferometric investigation of the ultrasonic-modulated fracture surface allows the study of the variation in the fracture plane (Fig. 31).

In this regard, we note that a crack bifurcation in a glass plate does not lead to any variation in fracture velocity (see Fig. 18). It is obvious that an interaction of the stresses of the two fractures takes place in this

case. The velocity remains, nevertheless, unchanged, even when the distance between the two cracks is small. Not even the formation of a cluster of fractures leads to a variation in velocity. This result seems to disagree with the decrease of fracture velocity sometimes observed between hackle marks. We must, however, keep in mind that a bifurcation occurs only when the tension in front of the fracture increases. At the origin of a bifurcation, there is, therefore, a surplus of elastic energy and no reason for the speed to decrease.

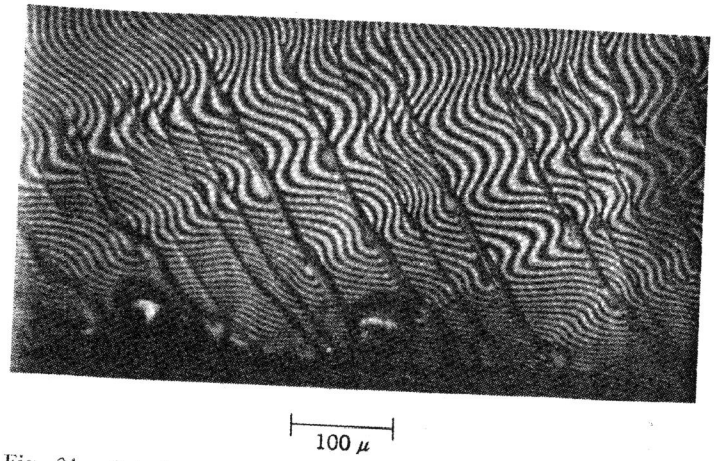

Fig. 31. Interference microscopic view of an ultrasonic-modulated lancet fracture. Light wavelength $\lambda = 0.54\ \mu$. Turning right of interference lines corresponds to face elevation. Fracture velocity: 320 to 550 m/sec.

Velocity Effects in Plastic Materials

In contrast to brittle materials, plastics do not show a well-defined maximum value of fracture velocity. The behavior in the initial phase is the same as is demonstrated in Fig. 8. The velocity increases to a constant value, too, but this value depends on the loading. For example, for the same type of Plexiglas (Alsthom), maximum values between 400 and 700 m/sec have been observed for different static tensions at the fracture origin; velocity increases with tension.

Still another effect must be mentioned: It often happens that several different maximum values are detected by the same experimental procedures. Figures 32 and 33 demonstrate two examples. Figure 32 shows the distance-time plot of a tensile test of Plexiglas. Only one fracture appears (Fig. 34). The fracture travels with two different values, 374 m/sec and 515 m/sec. Of course the real initial phase (which certainly exists) occurs earlier, but its run is too short, compared with the space resolution of the equipment and the breadth of the plate (100 mm), to be observed.

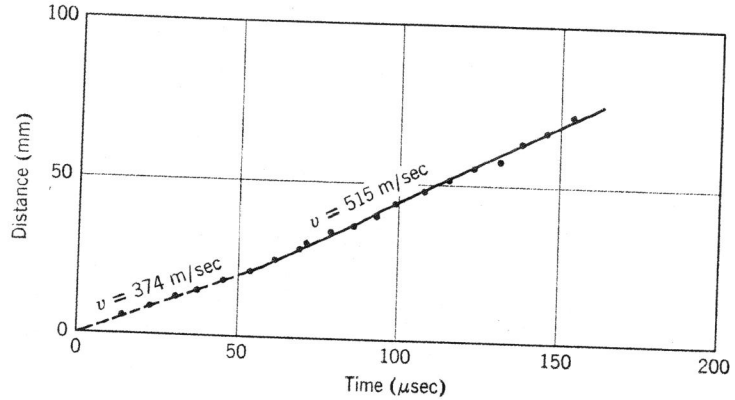

Fig. 32. Traveling fracture in Plexiglas.

Figure 33 gives another example. The main crack runs through the whole plate at a constant speed of 655 m/sec. At a distance of about 40 mm from the origin, a second crack is created by bifurcation. Its velocity is at first identical (655 m/sec). At a length of about 60 mm, a

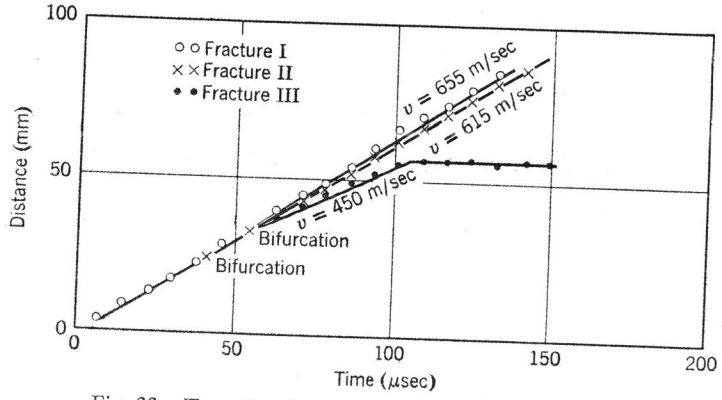

Fig. 33. Traveling fractures in Plexiglas, with bifurcations.

third crack starts, caused by another bifurcation. Simultaneously, the speed of the second crack slows down abruptly to 450 m/sec, while the third crack has nearly the same velocity as the first one (615 m/sec instead of 655 m/sec). At a total crack length of about 105 mm, the second fracture stops suddenly without any detectable decreasing zone (as described earlier in the discussion of brittle materials).

From these results it can be stated that in plastic materials different velocities occur, but each one, once it has appeared, is nearly stable. The reasons for this behavior are found in the plastic deformation in front of the fracture and the fact that rapid fractures in plastic materials are

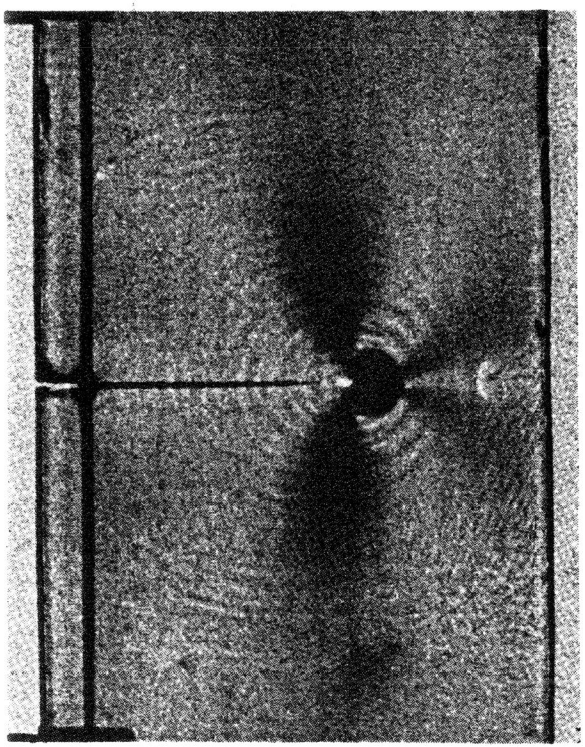

Fig. 34. Single picture of a traveling fracture in Plexiglas taken in a double-refraction setup. Tensile test.

usually created by a permanent formation of secondary cracks in front of the traveling fracture. The necessary stress is delivered by the stress corona surrounding the head of the fracture. The existence of hyperbolic lines in the fracture surface (Fig. 6) proves the theory. It is therefore evident that no well-defined constant maximum velocity can be observed. It seems, nevertheless, that some stabilizing effect might exist.

Velocity Effects in Plastic Foils

Two effects in foils have been investigated:[16,18,27] the bursting of plastic sheets and the tearing process under high-speed loading. Under

a tension stress of from 500 to 900 kg/cm² in the burst chamber, the fracture velocity in cellulose-acetate foils increases steadily from 500 to 800 m/sec, independent of foil thickness. This result indicates that surface effects are unimportant. In drawn sheets for which the tensile strength depends on orientation, tearing takes place normal to the direction of least strength. Strongly drawn sheets show a single fracture. Fracture velocity increases with the degree of drawing.

The tensile test was performed in an arrangement similar to that shown in Fig. 7. In the direction perpendicular to the direction of drawing, the fracture propagates more slowly by 1 or 2 orders of magnitude than in the direction of maximum speed. It can be expected that the further studies of fracture phenomena in foils will be very useful.

Conclusion

Among the different tools to measure fracture velocities, the multiple-spark camera and the ultrasonic technique are the most important.

In order to understand the physical phenomena controlling the fracture process, these techniques have been used to make speed measurements on different kinds and shapes of specimens under different loading and loading-speed conditions.

REFERENCES

Publications and documents about fracture by the following institutes:

Ballistic Institute, Berlin-Gatow (1935–1945)
Laboratoire de Recherches Techniques de Saint-Louis (LRSL) (1945–1958)
Department of Applied Physics at the University of Freiburg i. Br. (1950–1958)

1. H. Schardin and W. Struth, "Neuere Ergebnisse der Funkenkinematographie," *Z. tech. Physik*, **18,** 474 (1937).
2. H. Schardin and W. Struth, "Hochfrequenzkinematographische Untersuchung der Bruchvorgänge in Glas," *Glastech. Ber.*, **16,** 219 (1938).
3. H. Schardin, "Physikalische Vorgänge bei hohen Belastungen und Belastungsgeschwindigkeiten," Akademie für Lufsfahrtforschung (1938).
4. H. Schardin, D. Elle, and W. Struth, "Über den zeitlichen Ablauf des Bruchvorganges in Glas und Kunstglas," *Z. tech. Physik*, **21,** 393 (1940).
5. H. Schardin, "Ergebnisse der kinematographischen Untersuchung des Glasbruchvorganges," *Glastech. Ber.*, **23,** 1, 67, 325 (1950).
6. H. Schardin, "Über das Bruchkriterium bei kurzzeitiger Beanspruchung," *Glastech. Ber.*, **23,** 189 (1950).
7. A. Maue, "Uber das Auftreten von Sekundärbruchen beim Bruch von Gläsern," *Glastech. Ber.*, **23,** 336 (1950).
8. H. Schardin, "Kinematographische Auflösung des Zerreissvorganges," *Z. angew. Math. Mech.*, **31,** 261 (1951).
9. B. Bächle, "Die Biegefestigkeit von Tafelglas," Diplomarbeit, Freiburg (1952).

10. G. Hoffmann, "Über die Dispersion von Ultraschall in Platten," Staatsexamen, Freiburg (1952).
11. F. Kerkhof, "Analyse des Bruchvorganges spröder Körper mit Hilfe von Ultraschall," Freiburg (2/53).
12. W. Hoffmann, "Untersuchung von Stossvorgängen in festen Körpern," Freiburg (3/53).
13. G. Hoffmann, "Über die Ultraschall-Ausbreitung in Platten," Diplomarbeit, Freiburg (1953).
14. O. Horn, "Ein Verfahren zur Bestimmung von elastischen Konstanten fester Körper mittels Ultraschall," Diplomarbeit, Freiburg (1953).
15. F. Kerkhof, "Analyse des spröden Zugbruches von Gläsern mittels Ultraschall," *Naturwiss.*, **40,** 478 (1953).
16. H. Reichenbach, "Berstvorgang an Kunststoff-Folien," Freiburg (1/54).
17. H. Dreizler, "Analyse des Bruchvorganges mit Hilfe von Ultraschall," Freiburg (2/54).
18. H. Reichenbach, "Zusammenhang zwischen Reckgrad und Ultrarotabsorption bei Luvithern-Folien," Freiburg (3/54).
19. W. Hoffmann, "Untersuchung von Stossvorgängen in festen Körpern," Freiburg (5/54).
20. R. Quenett, "Über die Biegefestigkeit von Tafelglas in Abhängigkeit von der Plattengrösse und der Belastungsgeschwindigkeit," Diplomarbeit, Freiburg (1954).
21. H. Dreizler, "Eine Apparatur zum Zerreissen von Glasstaben im Ultraschallfeld," Diplomarbeit, Freiburg (1954).
22. H. Schardin, "Fracture Processes in Glass," *Proc. Intern. Comm. Glass*, **1,** 81 (1954).
23. H. Schardin, "Untersuchung von Zerreissvorgängen bei Kunststoffen," *Kunststoffe*, **44,** 48 (1954).
24. H. Schardin, L. Mücke, and W. Struth, "Bruchgeschwindigkeit von Gläsern," *Glastech. Ber.*, **27,** 141 (1954).
25. H. Schardin, "Die Anwendung der Funkenkinematographie zur Untersuchung von Bruchvorgängen," *Actes du 2ème Congrès Int. Phot. Ciném. Ultra-Rapides*, Paris, p. 301 (1954).
26. H. Hänsel and H. Schardin, "Ausbreitung elastischer und plastischer Oberflächendeformationen bei Metallen unter kurzzeitiger Belastung," *Actes du 2ème Congrès Int. Phot. Ciném. Ultra-Rapides*, Paris, p. 315 (1954).
27. H. Reichenbach, "Über den Berstvorgang von Kunststoff-Folien," *Actes du 2ème Congrès Int. Phot. Ciném. Ultra-Rapides*, Paris, p. 333 (1954).
28. H. Reichenbach, "Berst- und Zerreissvorgänge an Kunststoff-Folien," Freiburg (1/55).
29. F. Kerkhof, "Zusammenfassender Bericht über die Untersuchung von Berst-, Bruch- und Zerreissvorgängen," Freiburg (2/55).
30. H. Schardin and F. Kerkhof, "Ein neues Verfahren zur Bestimmung der Biegefestigkeit von Tafelglas," *Glastech. Ber.*, **28,** 124 (1955).
31. W. Hoffmann, "Ein Verfahren zur Messung geringer Laufzeitdifferenzen elastischer Wellen," Freiburg (1955).
32. F. Kerkhof, "Ein einfacher Versuch zur Bruchflächenmarkierung durch mechanische Impulse," *Glastech. Ber.*, **28,** 57 (1955).
33. F. Kerkhof, "Bruchuntersuchungen mit Hilfe von Ultraschall Vortrag Sitzung FA I," Frankfurt (1955).
34. F. Kerkhof, R. Seeliger, and W. Westphal, "Elektronenmikroskopische Untersuchungen an Opakglasbruchflächen," *Glastech. Ber.*, **28,** 262 (1955).

35. H. Schardin, W. Struth, and L. Mücke, "Bruchgeschwindigkeit einfach zusammengesetzer Gläser," LRSL Notice 28.3 (1956).
36. H. Hänsel and H. Schardin, "Ausbreitung von elastischen Oberflächendeformationen bei Stossbelastung fester Körper," *VDI Ber.*, **8,** 124 (1956).
37. H. Hänsel, "Zur Bruchgeschwindigkeit von Gläsern," LRSL (11a/1956).
38. H. Hänsel, "Über die Abhängigkeit der Bruchhöchstgeschwindigkeit fester Körper von der Körperschallgeschwindigkeit," LRSL (14a/1956).
39. F. Kerkhof and H. Dreizler, "Untersuchung des Bruchvorganges mittels Ultraschall," *Glastech. Ber.*, **29,** 459 (1956).
40. F. Kerkhof, "Ultrasonic Fractography," *Proc. 3rd Intern. Congress High-Speed Photography*, London, p. 194 (1956).
41. F. Kerkhof, "Zur theoretischen Deutung der maximalen Geschwindigkeit der Sprödbruchausbreitung," *Glastech. Ber.*, **30,** 365 (1957).
42. H. Hänsel, "Über die Bruchgeschwindigkeit von Gläsern als physikalische Stoffeigenschaft," LRSL (4/57).
43. F. Kerkhof, "Untersuchung über die Bruchfestigkeit des Glases und das ins Einzelne gehende Studium der Bruchvorgänge," Freiburg (2/57).
44. F. Kerkhof, "Zusammenfassender Bericht über die Untersuchung von Bruch- und Zerreissvorgängen," Freiburg (6/57).
45. F. Kerkhof and G. Manitz, "Stand der Untersuchung des Bruchvorganges an Plexiglas nach der Ultraschallmethode," Freiburg (8/57).
46. H. Schardin, "Kurzzeituntersuchungen an Kunststoffen," LRSL (4m/57).
47. F. Kerkhof, "Fraktographie mithilfe von Ultraschall," *Phot. u. Wiss.*, **1,** 13 (1958).
48. H. Hänsel, "Ergebnisse der HF-Kinematographie bei der Untersuchung der Sprödbruchfortpflanzung," *5th Intern. Congress High-Speed Phot.*, Köln (1958).
49. G. Manitz, "Untersuchung des Sprödbruchverlaufs von Polymeren mithilfe von Ultraschall," Freiburg (4/58).
50. F. Kerkhof and G. Manitz, "Bruchzeichnung durch interferierende Ultraschallwellen," *Glastech. Ber.*, **31,** 377 (1958).
51. F. Kerkhof, "Zusammenfassender Bericht über den Bruchvorgang," Freiburg (7/58).

Publications from other sources:

52. A. Smekal, *Österr. Ingr.-Arch.*, **7,** 49 (1953).
53. H. M. Dimmick, *J. Soc. Glass Technol.*, **35,** T318 (1951).
54. N. F. Mott, *Engineering*, **165,** 16, 53 (1948).
55. E. F. Poncelet, *Metals Technol.*, **11,** Technical Publication 1684 (April, 1944).
56. D. K. Roberts and A. A. Wells, *Engineering*, **178,** 820 (1954).
57. A. M. Bueche and A. V. White, *J. Appl. Phys.*, **27,** 980 (1956).
58. L. Ainsworth, *J. Soc. Glass Technol.*, **38,** 479 (1954).
59. E. W. Taylor, *J. Soc. Glass Technol.*, **34,** 69 (1950).

DISCUSSION

W. J. Hall, *University of Illinois.* Schardin's remarks concerning velocity effects in fracture are extremely interesting in the light of some of our recent work, particularly his comments concerning the decrease of the fracture velocity and the velocity effects in plastic materials. Some

of our recent observations arising from tests of wide steel plates may be of interest in this connection.

At the University of Illinois, measurements of surface strain and crack speed have been made as a brittle fracture traverses a wide steel plate. In $\frac{3}{4}$-in. thick by 6-ft wide plain steel plates tested by the notch wedge-impact method of fracture initiation at about 0°F and 19,000-psi average net stress, it has been found that the fracture velocity in the majority of cases is normally in the range of 2100 to 3900 fps. The fracture speed could be computed in two ways: (1) by knowing the time of breaking rather ductile, single-wire detectors glued to the surface of the plate, and the distance between these detectors, and (2) by knowing the time of maximum peak response of strain gages adjacent to the fracture path. Both methods of measuring fracture speeds gave reasonably consistent results, but they are cruder than the methods described by Schardin.

Some pilot studies of prestressed plates have been completed in which the edges of the plates are in tension (which helps initiation) and the central region is in compression. If the compression is not too great and does not arrest the crack, the fracture runs completely across the plate. In such cases, the fracture speed during the first portion of the run is of the same order of magnitude as that found for the plain plate tests, but, upon entering the compressive field, the fracture slows down and propagates at speeds as low as 100 fps, values as much as thirty to fifty times slower than those found in the plain plate test. This observation has been made in tests of both 2-ft wide and 6-ft wide plates of $\frac{3}{4}$-in. thick steel material, and further studies are currently under way. To all outward appearances, the fracture surfaces of the slow and fast fractures are identical, and in both cases they are brittle in nature. The fractures exhibit no evidence of momentary arrest, which, of course, could produce low average speeds.